Identification of Amino Acid Residues Photolabeled with 8-Azidoadenosine 5′-Diphosphate in the Catalytic Site of Sarcoplasmic Reticulum Ca-ATPase†

J.-J. Lacapère,*,‡ J. Garin,§ B. Trinnaman,∥ and N. M. Green∥

Section de Biophysique des Proteines et des Membranes (URA 1290 CNRS), Departement de Biologie Moleculaire et Cellulaire, CEN Saclay, 91191 Gif sur Yvette, France, Laboratoire de Biochimie (URA 1130 CNRS), Dêpartement de Biologie Molêculaire et Structurale, Groupement CEA-CNRS-INSERM-UJF, 85X, 38041 Grenoble Cedex, France, and Protein Structure, NIMR, The Ridgeway, Mill Hill, London NW7 1AA, United Kingdom

Received April 30, 1992; Revised Manuscript Received January 20, 1993

ABSTRACT: The photoreactive ADP analogue 8-N_3-ADP binds in the dark to the catalytic site of the sarcoplasmic reticulum Ca-ATPase. An apparent K_d value of 30 μM has been deduced from competition with ADP in the presence of EGTA. Photoirradiation of Ca-ATPase with 8-N_3-[^{3}H]ADP in the presence of calcium results in irreversible inhibition of ATPase activity with corresponding stoichiometries of covalently and specifically photolabeled Ca-ATPase. The site of photolabeling of the Ca-ATPase in the presence of calcium has been explored. Controlled trypsin digestion of the labeled protein shows that 8-azido-ADP is incorporated in the B subfragment. Extensive trypsin digestion of the labeled protein releases a small peptide as revealed by gel filtration chromatography (Sephadex G-50). Further HPLC purification on a reverse-phase column (C_8) eluted with a water/acetonitrile gradient buffered at pH 6 or at pH 2 gives a single labeled peptide. Edman degradation of that isolated peptide, as well as the amino acid composition, shows that it contains five amino acid residues (Val-530–Arg-534) with the radioactivity localized on Thr-532 and Thr-533.

The Ca-ATPase from the sarcoplasmic reticulum (SR)[1] is a transmembranous enzyme which couples the hydrolysis of an ATP molecule to the transport of two calcium ions across the membrane [for reviews, see De Meis (1981) and Inesi (1985)].

Elucidation of the structure of ATPase is an essential step toward the understanding of the molecular mechanism of coupling between calcium transport and ATP hydrolysis. The primary structure of SR ATPase was determined a few years ago, and a secondary structure prediction has been proposed (MacLennan et al., 1985; Brandl et al., 1986). More recently, three-dimensional crystals have provided good information on the shape of both cytoplasmic and transmembranous parts of the protein (Stokes & Green, 1990a,b). However, the knowledge of the actual folding of the peptide chain is still quite limited [for a review, see Green and Stokes (1992)]. Surface-exposed epitopes have been recently analyzed using polyclonal antibodies (Tunwell et al., 1991). Active-site mapping has been carried out by site-specific chemical modification of the ATPase molecule or more recently by site-specific mutagenesis. For instance, the mutagenesis has allowed the location of putative high-affinity calcium binding sites (Clarke et al., 1989a,b) and some of the amino acids making up the ATP binding site (Maruyama & MacLennan, 1988; Maruyama et al., 1989; Clarke et al., 1990; Vilsen et al., 1991). However, the knowledge of the amino acids directly involved in the adenine binding part of the catalytic site remains incomplete. Several years ago, it was shown that Asp-351 and Lys-515 are the phosphorylated and FITC reactive amino acids, respectively (Allen & Green, 1976; Mitchinson et al., 1982). More recently, Lys-492 and -684 have been shown to react with the terminal part of an ATP analogue, AP_3PL (Yamamoto et al., 1988, 1989). An Arg residue was also proposed to be part of the ATP binding site (Murphy, 1976; Bishop, 1989). In previous attempts at labeling SR Ca-ATPase by azido nucleotides, Briggs et al. (1980) first showed that Ca-ATPase was labeled with 8-N_3-ATP, a substrate for the enzyme, results confirmed later by several authors (Campbell & MacLennan, 1983; Shoshan-Barmatz, 1987). More recently, Seebregts and McIntosh (1989) covalently attached TNP-8N_3-ATP, a nonhydrolyzable analogue of ATP, to the catalytic site of the Ca-ATPase under conditions designed to favor the different forms of the site, and this year, McIntosh et al. (1992) localized Lys-492 as the modified amino acid.

In this paper, we describe the conditions required for labeling of the nucleotide binding site with 8-N_3-[^{3}H]ADP. After trypsin digestion, gel filtration, and reversed-phase HPLC, we identified a single radiolabeled peptide. Amino acid analysis and microsequencing showed that Thr-532 and Thr-533 are labeled. The structure of the catalytic site of the Ca-ATPase is discussed.

MATERIALS AND METHODS

SR vesicles have been prepared and protein concentrations have been determined as described in Champeil et al. (1985). All experiments have been carried out at pH 8.0.

8-N_3-[^{3}H]ADP was synthesized as follows: 12 mg of AMP was added to 5 mCi of [2-^{3}H]AMP and converted to 8-Br-[^{3}H]AMP with bromine water as described by Czarnecki et al. (1979). After 4 h at room temperature, the reaction mixture is neutralized by addition of 4 M NH_4OH, applied to a DE 52 (Whatman) column (1.5 × 30 cm), and eluted using a

† J.-J.L. was supported by a fellowship from the Royal Society.

‡ CEN Saclay.

§ CEN Grenoble.

∥ NIMR London.

[1] Abbreviations: SR, sarcoplasmic reticulum; SRV, SR vesicles; NH_4HCO_3, ammonium bicarbonate; AP_3PL, adenosine triphosphopyridoxal; 8-N_3-ADP/ATP, 8-azidoadenosine 5′-di/triphosphate; EGTA, ethylene glycol bis(β-aminoethyl ether)-*N,N,N′,N′*-tetraacetic acid; HPLC, high-performance liquid chromatography; K_d, dissociation constant; TFA, trifluoroacetic acid; Tricine, *N*-[tris(hydroxymethyl)methyl]glycine; Tris, tris(hydroxymethyl)aminomethane; TNP-ATP, 2′(3′)-*O*-(2,4,6-trinitrophenyl)adenosine 5′-triphosphate; TNP-8N_3-ATP, 8-azido-TNP-ATP.

0006-2960/93/0432-3414$04.00/0

linear gradient of 0–0.3 M triethylammonium bicarbonate (pH 7.4). The gumlike triethylammonium salt of 8-Br-[^{3}H]-AMP (15 μmol) was dried twice with anhydrous dimethylformamide on a rotavapor. 8-Azido[^{3}H]AMP was synthesized as described by Boos et al. (1978) by adding 150 μL of a 1 M solution of tetraethylammonium azide in dry DMF. After 1 night at 70 °C, the reaction mixture was applied to a DE 52 column and eluted using a linear gradient of 0–0.4 M triethylammonium bicarbonate, 1-L total volume. 8-Azido-[^{3}H]AMP was characterized by an A_{max} at 281 nm (ϵ = 13 300 at pH 7.0; Boos et al., 1978). Pure 8-azido[^{3}H]ADP was obtained from 8-azido[^{3}H]AMP by phosphorylation according to the method of Hoard and Ott (1965), using carbonyldiimidazole as the coupling reagent. Six micromoles of pure 8-azido[^{3}H]ADP was obtained after purification with a DE 52 column eluted with a 2-L linear gradient of 0–0.5 M TEA-HCO_3 (pH 7.4).

Binding Measurements. ADP-induced fluorescence changes were measured as described in Lacapère et al. (1990). 8-N_3-ADP from Sigma was used for competition experiments, and changes in the absorbance at 295 nm were compensated by changing the gain.

[^{14}C]ADP was used to measure the stoichiometry of nucleotide binding sites by filtration on Millipore filters as described in Lacapère et al. (1990).

The amount of 8-N_3-[^{3}H]ADP covalently bound was measured as follows: an aliquot (50 μL) of SRV (1 mg/mL) preincubated with azido-ADP and irradiated for 1 min with a xenon lamp (150 W) at 0 °C was filtered on a 0.45-μm Millipore filter and washed with an excess of the same buffer completed with ADP. The remaining ATPase activity was measured on the same sample as described in Lacapère et al. (1990). We checked that irradiation had no effects on the protein by assaying ATPase activity before and after irradiation.

Electrophoresis gels were carried out as described in Torok et al. (1988). Gels were cut into 0.5-cm slices, incubated at 60 °C overnight in 0.6 mL of 30% w/v hydrogen peroxide, and counted.

Derivatization. Two chemical modifications of labeled SRV were done prior to cleavage: carboxymethylation was performed to block cysteine residues, and succinylation of lysines was performed to block them and to unfold the protein. Iodoacetic acid (IAA/SRV = 400/1 M/M) was added and the pH adjusted to 8.0 if needed. After 20-min incubation at room temperature, powdered succinic anhydride (SA/SRV = 2/1 w/w) was added slowly and the pH maintained at 8.0 by addition of NaOH. After 20 min at room temperature, iodoacetic acid treatment was repeated.

Protein Cleavage. Trypsin treatment was performed as follows: modified and labeled SRV were centrifuged (30 min, 40 000 rpm in a 50 Ti rotor) and resuspended in 50 mM Tricine–Tris (pH 8.0)/1 mM $CaCl_2$ with 1/50 (w/w) trypsin/protein and incubated 1 h at 37 °C. Reaction was stopped by addition of a 2-fold excess of trypsin inhibitor.

CNBr treatment was performed on unmodified enzyme as follows: labeled SRV were centrifuged (30 min, 40 000 rpm in a 50 Ti rotor) and resuspended in 80% formic acid. A 10-fold excess of CNBr over protein was added, and cleavage was performed overnight at room temperature in the dark under nitrogen. Reaction was stopped by addition of a 100-fold excess of cold water, and the volume was reduced to 1 mL. This was repeated twice before any fractionation.

Peptide Purification. Peptides from the above digest were fractionated by gel filtration and by HPLC.

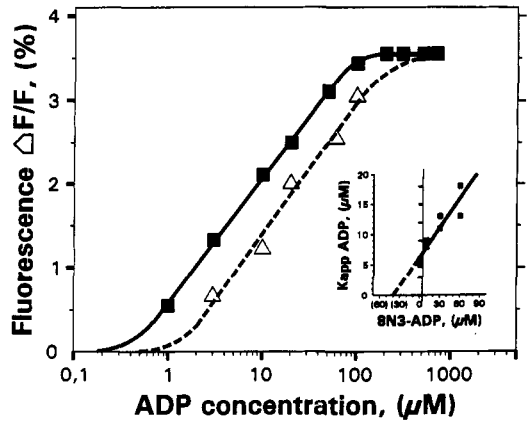

FIGURE 1: ADP dependence of fluorescence changes at various 8-N_3-ADP concentrations in the absence of calcium. Fluorescence conditions are described under Materials and Methods. The medium was adjusted to pH 8.0 by 200 mM Tricine–Tris in the presence of 0.2 mM EGTA–Tris. Data were corrected for dilution plus absorption of the excitation light by nucleotide at 295 nm. Inset: 8-N_3-ADP concentration dependence of the dissociation constant of ADP binding. The dashed line shows the extrapolated value of the inhibition constant of 8-N_3-ADP.

Gel filtration was performed on Sephadex G-50 (superfine grade) at room temperature. The column size was 1.6 cm × 90 cm, the buffer was 50 mM NH_4HCO_3 (pH 8.5), the flow rate was 12 mL/h, and the fractions were 2 mL in size. Fractions from the column were assayed for UV absorption at 215 nm and for radioactivity by liquid scintillation. Fractions were pooled according to the radioactivity profile and freeze-dried.

HPLC was performed using Beckman equipment with a Zorbax reverse-phase C_8 column (0.46 × 15 cm); peptides were fractionated using a water/acetonitrile gradient (0–90%) buffered either at pH 6 with ammonium acetate or at pH 2 with TFA (14 mM or 0.1% and 10 mM or 0.09% for ammonium acetate and TFA, respectively, in 100% water and 90% acetonitrile).

Peptide Sequencing. Sequence analysis was performed by Alan Harris with Applied Biosystems 470A gas-phase and 477A pulse liquid-phase peptide sequenators. PTH-amino acids were analyzed on-line with Applied Biosystems 120A analyzers. Data collection and analysis were achieved with an Applied Biosystems 900A module calibrated with 25 pmol of PTH-amino acid standards (Toker et al., 1990). Forty percent of the PTH-amino acid which remained in the fraction collector was used for radioactivity counting. The peptide sequenced was first covalently coupled to a Sequelon arylamine (AA) filter using the standard procedure described by Millipore.

Amino Acid Analysis. This was carried out by Fatima Beg using an Applied Biosystems 420A derivatizer–analyzer fitted with an on-line 130A phenylthiocarbamoyl analyzer. Peptides were hydrolyzed for 20–24 h at 110 °C with 6 M HCl/2 mM phenol in the vapor phase under nitrogen. Samples were dried, dissolved in distilled water, and lyophilized before analysis (Toker et al., 1990). PTC-amino acids coming out of the analyzer were collected for counting.

RESULTS

Binding of 8-N_3-ADP without Illumination. Binding of ADP to the Ca-ATPase in the presence of EGTA enhances the intrinsic fluorescence (Figure 1), which enabled us to deduce a K_d of 5–6 μM for ADP binding (Lacapère et al., 1990). From competition between 8-N_3-ADP and ADP, a K_i

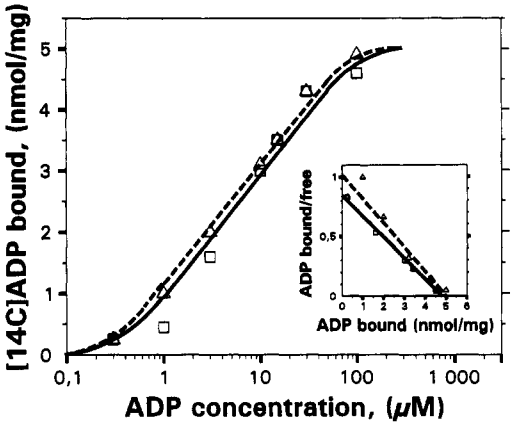

FIGURE 2: ADP concentration dependence of [^{14}C]ADP binding in the presence or in the absence of calcium. The medium was 200 mM Tricine–Tris, pH 8.0, in the presence of either 0.1 mM $CaCl_2$ (triangles) or 0.2 mM EGTA–Tris (squares). Inset: Scatchard plot of the binding data.

Table I: [^{14}C]ADP = 10 μM

	[^{14}C]ADP bound		
SRV (mg/mL)	nmol/mL	nmol/mg	sites occupied (%)
0.2	0.56	2.8	56
0.5	0.9	1.8	36
1.0	1.65	1.65	33

of 30 μM for 8-N_3-ADP was calculated (see inset of Figure 1). Binding of [^{14}C]ADP was also measured by filtration in the presence of both EGTA and Ca. Similar K_d values of 5–6 μM are measured in both conditions with a similar stoichiometry (5 nmol/mg) as revealed by the Scatchard plot (Figure 2 and inset of Figure 2). It should be noted that unlike ADP and for unknown reasons 8-N_3-ADP did not enhance the intrinsic fluorescence when bound to SRV preincubated in EGTA.

To achieve a good level of covalent binding of 8-N_3-ADP by illumination, the half-time of the protein–ligand complex should not be less than the lifetime of nitrene. Therefore, we checked the best conditions and measured the dissociation rate constant of [^{14}C]ADP by rapid filtration. When incubated in the presence of calcium, k_{off} was 10 s^{-1}, whereas it was too fast for the technique when incubated in the presence of EGTA (data not shown). This result is consistent with previous experiments showing a faster dissociation rate constant for Mg·ATP in the presence of EGTA compared to Ca (Lacapère & Guillain, 1992). Thus, it was decided to include calcium in the photolabeling medium.

Due to low amount of 8-N_3-[^{3}H]ADP available, we checked the nucleotide and protein concentration ratio yielding the highest amount of nucleotide bound. Table I shows that at constant nucleotide concentration in a small volume, an increase in protein concentration reduces the stoichiometry of bound nucleotide (nanomoles per milligram) but increases the total amount of bound nucleotide (nanomoles per milliliter).

Binding of 8-N_3-[^{3}H]ADP upon Illumination. In the presence of calcium, the stoichiometry of covalently bound 8-N_3-[^{3}H]ADP has a maximal value of 1.2 nmol/mg (Figure 3). This is lower than the 5 nmol/mg of nucleotide binding sites measured with ADP (Figure 2) which can be due to the yield of labeling (25%) but also to the substrate/protein ratio. In fact, Table I shows that an increase of protein concentration at a constant ADP concentration induces an increase of the amount of ADP bound (nanomoles per milliliter) but a decrease of the stoichiometry (nanomoles per milligram).

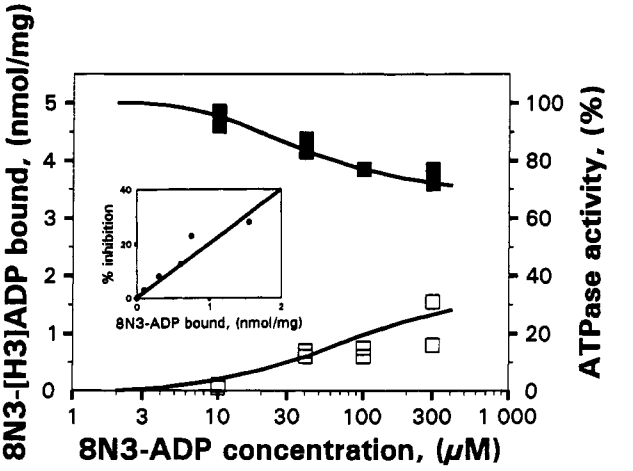

FIGURE 3: [8-N_3-ADP] dependence of 8-N_3-[^{3}H]ADP binding (open squares) and ATPase activity (closed squares). Experimental conditions are described under Materials and Methods. The medium was adjusted at pH 8.0 with 200 mM Tricine–Tris in the presence of 0.1 mM $CaCl_2$. Inset: Relation between 8-N_3-[^{3}H]ADP incorporation and inhibition of ATPase activity.

However, the yield of labeling is good in conditions of exchange between bound and free nucleotide. Figure 3 also shows that corresponding measurements of ATPase activity after illumination in the presence of 8-N_3-[^{3}H]ADP present a pattern similar to the covalent binding. The inset in Figure 3 shows that extrapolation to complete inhibition of the ATPase activity corresponds to the binding of 1 mol of azido-ADP/mol of active site, since it reaches a stoichiometry of 5 nmol/mg, equal to the maximal stoichiometry of ADP bound (Figure 2). In the presence of calcium, half-saturation of covalently bound 8-N_3-[^{3}H]ADP and half-inhibition of ATPase activity are reached at 40 μM azido-ADP (Figure 3), a value similar to the one deduced from competition with ADP in the presence of EGTA (Figure 1).

Exploration of Covalent Binding of 8-N_3-[^{3}H]ADP. Figure 4 shows electrophoresis gels of labeled SR, without any cleavage and with partial cleavage with trypsin. Panel A and the first gel show that most of the labeling was on the Ca-ATPase. Controlled tryptic cleavage led to the formation of the primary tryptic fragments A and B after cleavage at the T_1 site (Torok et al., 1988). The second gel and panel B show tryptic cleavage performed at a 1/100 ratio (trypsin/SRV) and the corresponding radioactivity profile; it confirms the labeling of Ca-ATPase, since a major radioactive band appears for molecular weights corresponding to the A and B fragments. The third gel and panel C (trypsin/SRV = 1/50) show the absence of any labeling at molecular weights corresponding to the A1 and A2 fragments observable with Coomassie blue; therefore, it appears that the B fragment has been labeled. It is noteworthy that the B fragment is also cleaved by trypsin treatment, thus explaining the displacement of the radioactivity peak between panels B and C.

It is worth mentioning that in order to count tritium efficiently it was necessary to solubilize the gel slices with H_2O_2 (see Materials and Methods).

Identification of Photolabeled Peptide. After photolabeling of Ca-ATPase with 8-N_3-[^{3}H]ADP, the enzyme was succinylated and carboxymethylated before trypsin cleavage as described under Materials and Methods. The cleavage products were subjected to fractionation by filtration on Sephadex G-50 equilibrated with 50 mM ammonium bicarbonate (Figure 5). The UV profile was similar to that reported by Allen (1980); the first peak corresponds to membranous

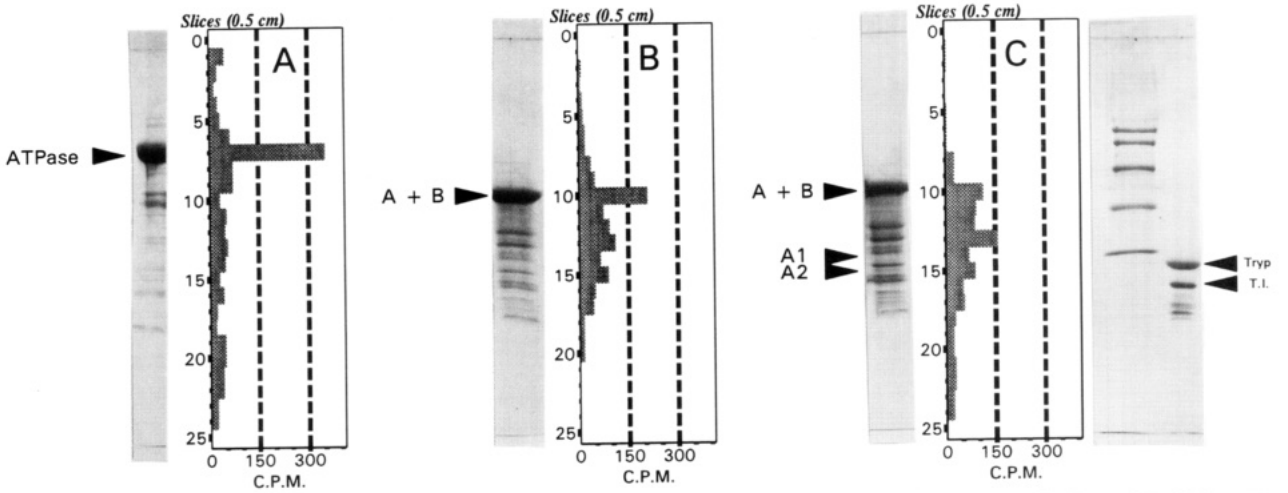

FIGURE 4: Photolabeling of Ca-ATPase with 8-N_3-[^{3}H]ADP and identification of photolabeled fragments. SDS–PAGE of Ca-ATPase membranes before tryptic cleavage (panel A) or after tryptic cleavage (panels B and C) at 1/100 and 1/50 trypsin/SRV, respectively. Standards are from Sigma.

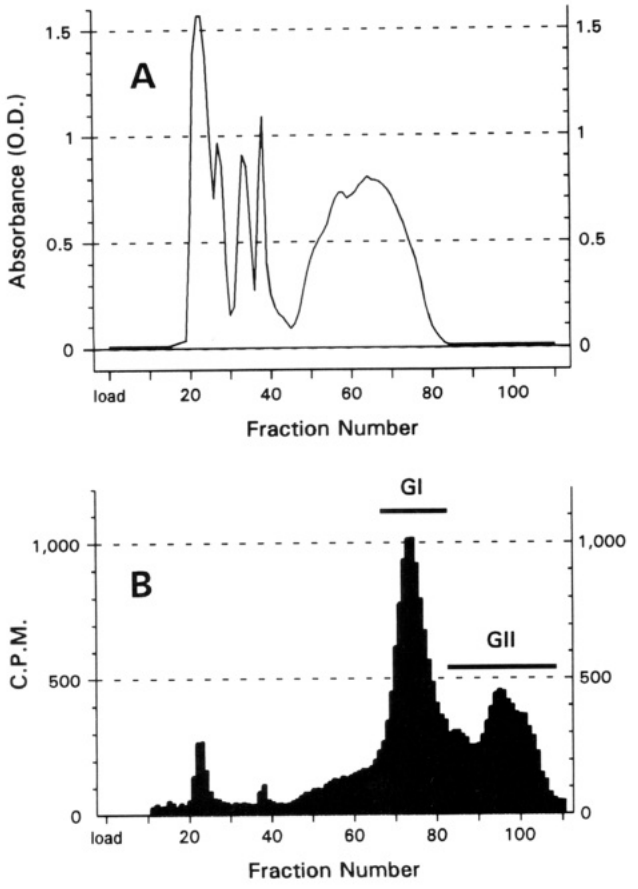

FIGURE 5: Separation of peptides from the tryptic digest of Ca-ATPase photolabeled with 8-N_3-[^{3}H]ADP on a column of Sephadex G-50 (superfine grade). The column size was 1.6 × 90 cm, and the buffer was 50 mM ammonium bicarbonate. Two-milliliter fractions were collected at a flow rate of 12 mL/h. (A) and (B) are respectively UV and radioactivity profiles. The horizontal bars indicate the pooled fractions (GI and GII).

fragments (void volume); the second, the third, and the fourth correspond to large soluble peptides (Green and Toms, unpublished results). The following massif is more complex: it contains small peptides and the total column void volume where salts are. The main peak in the radioactivity profile (fractions 67–82, GI) corresponds to unbound 8-N_3-[^{3}H]ADP and probably its breakdown products which come out in the total column volume. The first two small peaks (fractions 20–25 and 37–38) correspond to undigested protein and large peptides; the last radioactive peak (fractions 83–110, GII) should correspond to small labeled peptide more retained because of the presence of bound ADP and coming out after the total column void volume. Fractions were pooled according to the radioactivity profile (fractions GI and GII) as shown in Figure 5.

Instead of trypsin cleavage, we checked CNBr treatment followed by gel filtration chromatography. It gave a radioactivity peak attributed to the labeled peptide coming out earlier in the G50 elution profile (data not shown), meaning that the CNBr-cleaved labeled peptide is larger than the tryptic-labeled peptide.

The material of the two radioactive peaks (fractions GI and GII) obtained by fractionation of the tryptic digest on Sephadex G-50 was subjected to HPLC using a gradient of acetonitrile buffered at pH 6 with ammonium acetate (Figure 6). Fraction GI gave a major peak with 80% of the radioactivity eluted before the gradient of acetonitrile (Figure 6A), the remaining radioactivity being spread out along the other fractions. Fraction GII gave an HPLC profile more complex (see Figure 6B): three main peaks eluted before the gradient, one of which has a retention time consistent with the one observed for fraction GI. The two others have been analyzed either on sequencing with no sequence coming out or on amino acid analysis with also no peptide. These three peaks correspond to unbound nucleotide and breakdown products (probably due to glycosyl bound breakage upon irradiation), since a similar HPLC profile (three main peaks) was obtained when the labeling medium was analyzed, i.e., the supernatant of centrifugation performed after photolabeling and derivatization, as described under Materials and Methods (data not shown). Figure 6B also shows a peak eluted with the acetonitrile gradient (fractions 38–41). The amino acid composition of the fractions corresponding to this peak is presented in Table II; eight amino acids (Gly, Arg, Thr, Ala, Val, Ile, Leu, and Lys) are present in high amounts compared with other residues. The radioactivity profile reveals the presence of a radioactive peak coming out early in the elution before any standard amino acid, and it can be associated with a modified amino acid. Amino acid analysis clearly shows the need of further purification since no clear sequence emerged from these data.

Site of Covalent Attachment of 8-N_3-[^{3}H]ADP. The radioactive peak eluted with the acetonitrile gradient in Figure

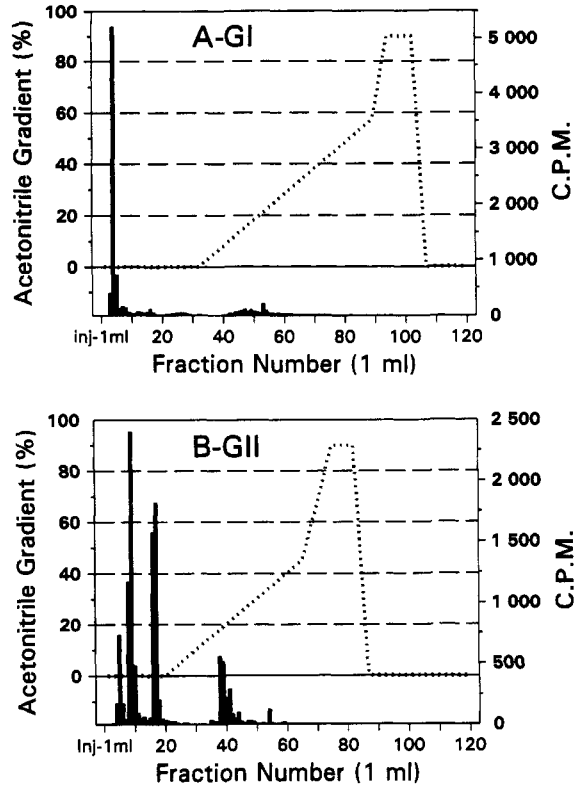

FIGURE 6: Purification of peptides from the two fractions GI (A) and GII (B) on a reverse-phase column by HPLC. The radioactive fractions pooled from Sephadex G-50 chromatography were freeze-dried and then redissolved in a small volume of distilled water. The samples were applied to a Zorbax C_8 column equilibrated in 100% buffer A [14 mM ammonium acetate buffer (pH 6) in water] and then eluted with a linear gradient of buffer B [10 mM ammonium acetate (pH 6) in 90% acetonitrile/10% water] at a flow rate of 1 mL/min. One-milliliter fractions were collected.

Table II: Amino Acid Composition of Fractions Pooled from the HPLC Experiment (Figure 6B, Peak Coming Out at 18–19% Acetonitrile) Buffered at pH 6[a]

amino acid residue	pmol	cpm	amino acid residue	pmol	cpm
unknown	(1)	2000	Ala	209	
Asp			Pro	59	
Glu	68		Tyr	41	
Ser	9		Val	100 (1)	
Gly	517 (1)		Met	11	
His			Ile, Leu	182	
Arg	110 (1)		Phe	70	
Thr	100 (1)		Lys	125	

[a] The amount of peptide used for amino acid analysis was 60 pmol, as estimated from the radioactivity. Numbers in parentheses are the estimated amino acids in the labeled peptide deduced from sequence analysis.

6B was subjected to HPLC using a gradient of acetonitrile buffered at pH 2 with TFA. Figure 7 shows the radioactivity profile of this HPLC rerun; a single peak appears at the beginning of the gradient. The peptide collected from the second HPLC purification (Figure 7) was covalently attached to a Sequelon AA filter before sequencing as described under Materials and Methods. Edman degradation of that immobilized peptide gave the following sequence: VGTTR corresponding to a fragment localized at positions 530–534 in the overall protein sequence (MacLennan et al., 1985). The amount of peptide covalently attached to the filter was too small (30 pmol) to give precise localization of the amino acid labeled within that sequence. However, the radioactivity profile of the released amino acids would be consistent with

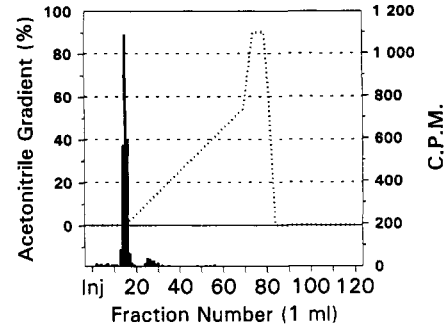

FIGURE 7: Further purification of the 8-N_3-[^{3}H]ADP-labeled peptide. The radioactive peak fractions (38, 39) obtained on HPLC from a previous purification (Figure 6) were applied to a Zorbax C_8 column equilibrated in 100% buffer A [0.1% TFA buffer (pH 2) in water] and then eluted with a linear gradient of buffer B [0.09% TFA buffer (pH 2) in 90% acetonitrile/10% water] at a flow rate of 1 mL/min. One-milliliter fractions were collected.

the Thr labeled, i.e., Thr-532 and Thr-533 (not shown). We compared this result with amino acid analysis done on less purified fractions and presented in Table II. The data are consistent with the sequences obtained from Edman degradation (see numbers in parentheses) and with labeled Thr since the amount of Thr is smaller than expected. Moreover, the early elution of this radioactive peak would fit with it being the ADP-labeled amino acid residue because of the high polarity of the phosphate groups. It is noteworthy that the labeled amino acids are localized within a portion of the protein which should give a longer peptide when treated with CNBr (25 amino acids) compared with trypsin (5 amino acids). This is in agreement with our data showing different Sephadex G50 elution profiles for trypsin cleavage and CNBr treatment. Further purification by HPLC of the radioactive peak obtained by fractionation on Sephadex G50 of the CNBr-treated protein gave a single radioactive peak (data not shown). For unknown reasons, it was impossible to get a sequence, whereas the amino acid composition of this peak (data not shown) gave all the amino acids present in the expected sequence which contains the tryptic region identified.

DISCUSSION

In the present study, we show that 8-N_3-ADP binds to the nucleotide binding site of the SR Ca-ATPase, as revealed by competition experiments done with ADP (Figure 1). The K_d value for 8-N_3-ADP, obtained by extrapolation in Figure 1, is slightly lower (6-fold) than the K_d value measured for ADP under similar conditions. The presence of a nitrene group can be the main cause of such a decrease, since a similar observation has been observed with TNP-AXP and their azido derivatives (Seebregts & McIntosh, 1989). In the latter case, the decrease in affinity is smaller (3-fold), and this can be explained by the presence of the TNP group which accounts by itself for a 30-fold increase in affinity of TNP-ATP relative to ATP (Dupont et al., 1985). The lower affinity for the 8-N_3-adenine nucleotides may also be a consequence of their syn conformation predominant in solution, differing from the conformation of ATP bound to the Ca-ATPase catalytic site (Clore et al., 1982) or 8-N_3-ADP bound to the F_1-ATPase catalytic site (Garin et al., 1988). However, 8-Br-ATP, which has also been postulated to be in the syn conformation in solution, was shown to be a good substrate for the Ca-ATPase and exhibit the same affinity as ATP (Champeil et al., 1988). Another interesting observation is that binding of 8-N_3-ADP did not enhance the fluorescence of the Ca-ATPase as previously observed for 8-Br-ATP (Champeil et al., 1988). This effect

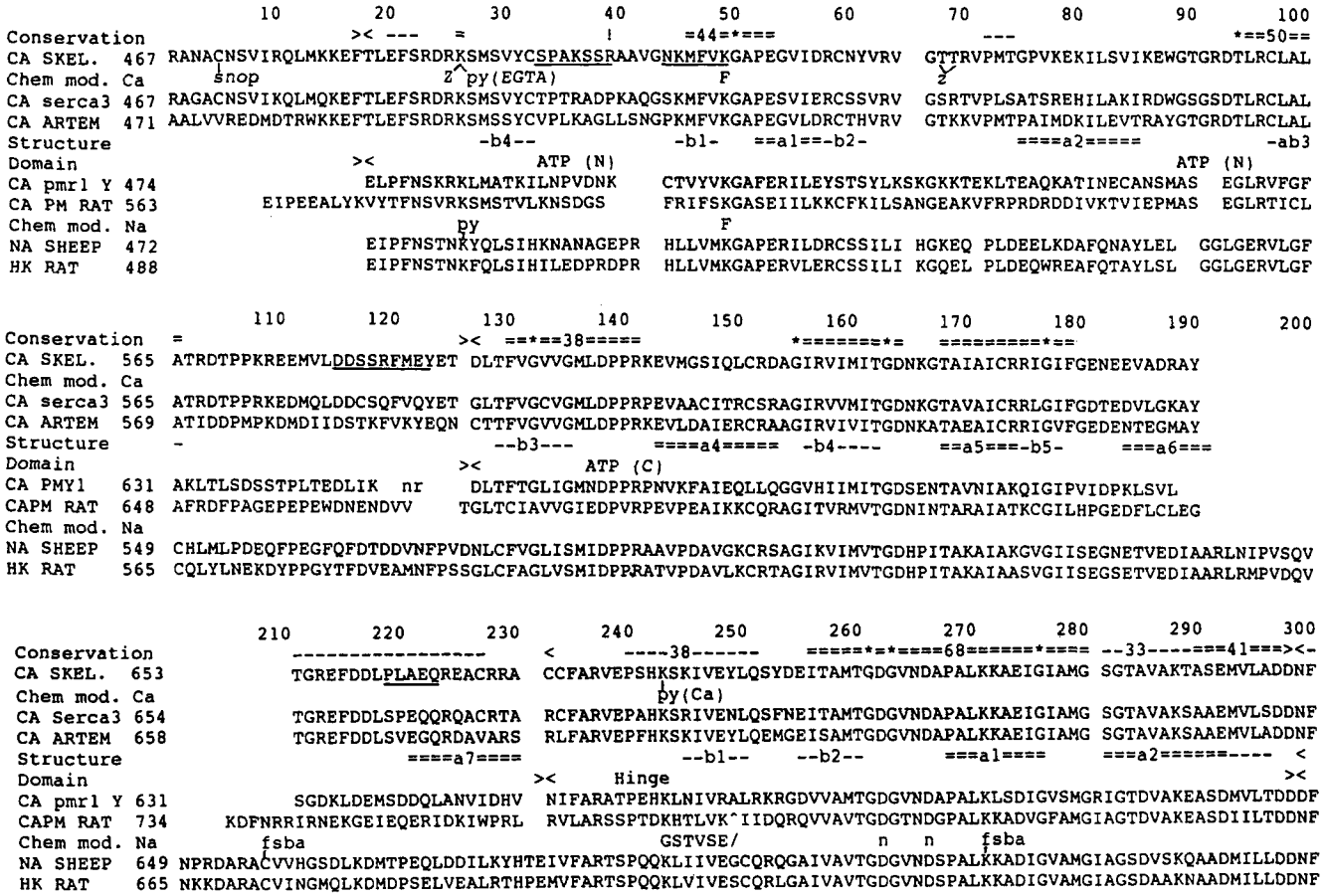

FIGURE 8: Aligned sequences of the nucleotide binding and hinge regions of Ca^{2+}-Na^+ and H^+ pumps. The sequences can be found in the Swissprot data base using the following designations: atcb rabit (Brandl et al., 1986); atcf rat (Burke et al., 1989); atcb artsa (Palmero & Sastre, 1989); atcl yeast (Rudolph et al., 1989); atcp rat (Shull & Greeb, 1988); atnl sheep (Shull et al., 1985); atha rat (Shull & Lingrel, 1986). Line 1, conserved regions (= = =, - - -) including glycine residues (*). Line 3, sites of affinity labeling in the skeletal Ca pump. Line 6, consensus secondary structure (= = a = =, α helix; - -b- -, β strand). Line 7, domain assignments. Line 10, sites of affinity labeling in the Na^+ pump. Abbreviations: F, fluorescein isothiocyanate; FSBA, [(fluorosulfonyl)benzoyl]adenosine; *n*, ClRATP (Ovchinikov et al., 1987); py, ATP pyridoxal; sno, thioinosine triphosphate; z, 8-azido-ADP; Z, 8-azido-TNP-ATP.

of 8-Br-ATP was suggested to be due to a quenching effect of the bromine on a neighboring tryptophan residue (Trp-552). However, the azide, bound in the same position on the adenine ring, does not appear to be capable of a quenching effect. An indirect effect of the azido group on the protein conformation seems more probable and consistent with the decrease in the amplitude of the superfluorescence observed when changing from TNP-ATP to its azido derivatives (Seebregts & McIntosh, 1989).

An important aspect of our results is that specific and efficient covalent labeling of the catalytic site occurs on irradiation (Figures 3 and 4). The pH and temperature dependence of labeling was described previously by others authors (Seebregts & McIntosh, 1989; Briggs et al., 1980) as well as the protecting effects of ATP and ADP against labeling (Briggs et al., 1980). It seems possible that our stoichiometry of labeling with 8-N_3-ADP, which correlates with the percentage inactivation of ATPase activity, is higher than those described previously for the Ca-ATPase with other 8-N_3-AXP nucleotides (Briggs et al., 1980; Lord & Richards, 1981; Campbell & MacLennan, 1983; Cable & Briggs, 1984; Shoshan-Barmatz, 1987), because of our experimental conditions (pH 8, 0 °C, and in the presence of Ca) combined with the choice of a nonhydrolyzable nucleotide.

The evidence for specific labeling of the catalytic site arises from the gel of the undigested protein (Figure 4) and from peptide purification (Figure 6). It is worth mentioning that, in our hands, the purification of labeled peptide after trypsin cleavage requires a preliminary fractionation on Sephadex G-50 equilibrated with NH_4HCO_3; otherwise, no radioactive HPLC peak was obtained (data not shown) possibly because of irreversible adsorption caused by charged phosphate groups; the ion pairing with ammonium bicarbonate may be stronger than adsorption and assist the desorption from the C_8 column matrix. Purification of the trypsin-cleaved labeled protein needs at least three steps: filtration followed by two HPLC runs on a reverse-phase column eluted with acetonitrile gradients buffered at pH 6 and 2. The amino acid composition of a radioactive fraction obtained from the first HPLC run clearly shows the need for further purification (Table II). However, analysis of the amino acid composition and of the corresponding radioactivity profile enabled us to suggest, at this stage, that within the sequence obtained after total purification (VGTTR), Thr residues are labeled, probably on their nucleophilic OH.

It should be noted that in a previous study, when Allen (1980) purified the soluble tryptic peptides from succinylated and carboxymethylated protein, the VGTTR peptide was localized in fractions coming out before the total column void volume of Sephadex G50. Therefore, the elution of 8-azido-labeled peptide VGTTR in fractions coming out after the total column void volume (this work) might be explained by strong interactions between the 8-azido-ADP moiety and the G50 gel support.

This sequence (VGTTR) is localized within the B subfragment of the Ca-ATPase and is part of a predicted loop

between a β strand and an α helix in the nucleotide binding site (Taylor & Green, 1989). The main problem in this model is that there are now four bends which appear to be close to the nucleotide site, in addition to those in the phosphorylation site and the hinge region. It is likely that some revision of the strand arrangement is needed, but it requires more data to provide a more firmly based structure. The VGTTR segment is conserved only in the ER calcium pump; in the sodium pump, only the glycine residue forming the nucleus of a bend is present. An improved alignment of this region is shown in Figure 8 emphasizing the common hydrophobicity pattern in the succeeding α helix. This segment differs from the proposed location of the TNP-8N_3-ATP label on the A1 subfragment, Lys-492 (McIntosh et al., 1992), and from the proposed location of the 8-N_3-ATP label on the Na/K-ATPase (Tran et al., 1988). In the latter cases, the covalently modified peptides are similar according to the alignment of the ATPase sequences (Green, 1989), although the labeling conditions were different. However, Seebregts and McIntosh (1989) pointed out that the level of catalytic site labeling changes depending on the experimental conditions, but also on the enzyme conformation. This has also been observed with another nonhydrolyzable ATP analog, adenosine triphosphopyridoxal (AP_3PL), which labeled different amino acids in the presence and in the absence of calcium (Yamamoto et al., 1988, 1989). Therefore, the discrepancy between our results and the earlier ones may be explained by a difference in the enzyme conformation or in the substrate conformation (8-N_3-ADP in our case and TNP-8N_3-AXP or 8-N_3-ATP in the other cases). Moreover, we have to take into account that several amino acids are probably close to the nucleotide within the catalytic site, only a few of which are really essential for recognition and activity.

Information about the amino acids involved within the catalytic site structure is available from either covalent modifications (Allen & Green, 1976; Mitchinson et al., 1982; Saïto et al., 1987; Bishop et al., 1988; Yamamoto et al., 1988, 1989; Kison et al., 1989; Seebregts & McIntosh, 1989; McIntosh, 1992) or mutagenesis [for a review, see McLennan (1990)]. Some distance measurements between covalently bound probes within the cytoplasmic domain of the Ca-ATPase have recently permitted a tentative description of the spatial arrangement of these probes (Bigelow & Inesi, 1991). Moreover, recent immunological experiments have defined some surface-exposed epitopes (Tunwell et al., 1991), reducing the number of possibilities for the spatial arrangement of amino acids. All these data, including this work, led us to propose an approximate model (see Figure 9).

A complete structure prediction of the catalytic site requires an analysis of the possible structure of the ATP molecule within the catalytic site. For the Ca-ATPase, Clore et al. (1982) show that the glycosyl bond linking the adenine base to the ribose sugar is in the anti conformation and that the ribose ring is N-type. More recently, NMR studies on ATP bound to the Na/K-ATPase show that the nucleotide is U-shaped with the cation above and approximately planar with the adenine ring (McD Stewart et al., 1989). This structure of the ATP is consistent with another recent NMR study of the ATP molecule in solution (Andre et al., 1990) but differs from the more extended structure of GTP observed within the crystals of the Ha-Ras p21 protein (Schlichting et al., 1990) which may have a completely different catalytic site, since a covalent phosphoenzyme is not formed.

Finally, we anticipate that covalent labeling with a wide variety of photoaffinity nucleotide probes or chemical reagents specific for a class of amino acids combined with the structure of the metal–ATP complex may define a tertiary structure of the catalytic site of the Ca-ATPase.

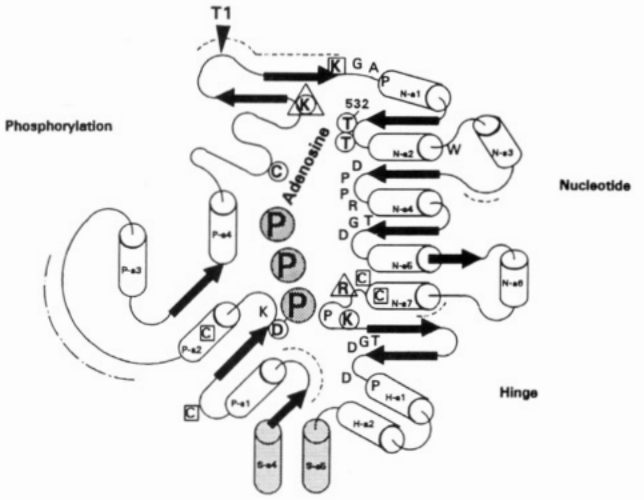

FIGURE 9: Two-dimensional layout of the secondary structure element of the kinase region of the Ca^{2+}-ATPase. No attempt has been made to reconstruct the 3-D relationship, but the arrangement is realistic to the extent that conserved bends at the C-termini of β strands are brought close to the central ATP ligand. The sites in the hinge and phosphorylation regions, which are labeled by activated "γ-phosphate reagents", are appropriately close to the δ-phosphate, and the adenine is close to residues labeling by azidoadenosine nucleotides (amino acids within circles). However, K_{492} and R_{678} (within triangles), which are cross-linked by glutaraldehyde (McIntosh, 1992), are not close together. Residues which lead to loss of transport when mutated are also shown in capital letters. Amino acids within squares are those used for distance measurements between covalently bound probes (Bigelow & Inesi, 1991). Regions which are epitopes of mono- or polyclonal antibodies are shown with a dotted line. Details of labeling reagents, sequence context, and site conservation can be found by reference to the alignment (Figure 8).

ACKNOWLEDGMENT

We gratefully acknowledge A. Aitken for helpful discussions and P. V. Vignais for his contribution. We also thank A. Harris and F. Beg for their assistance with sequencing and amino acid analysis.

REFERENCES

Allen, G. (1980) *Biochem. J. 187*, 545–563.
Allen, G., Green, N. M. (1976) *FEBS Lett. 63*, 188–192.
Andre, F., Demassier, V., Bloch, G., & Neumann, J. M. (1990) *J. Am. Chem. Soc. 112*, 6784–6789.
Bigelow, D. J., & Inesi, G. (1991) *Biochemistry 30*, 2113–2125.
Bishop, J. E. (1989) *Biophys. J. 55*, 204a.
Bishop, J. E., Squier, T. C., & Bigelow, D. J. (1988) *Biochemistry 27*, 5233–5240.
Boos, K. S., Bridenbaugh, R., Ronald, R., & Yount, R. G. (1978) *FEBS Lett. 91*, 285–288.
Brandl, C. J., Green, N. M., Korczak, K., & MacLennan, D. (1986) *Cell 44*, 597–607.
Briggs, F. N., Al-Jumaily, W., & Haley, B. E. (1980) *Cell Calcium 1*, 205–215.
Burke, S. E., Lytton, J., MacLennan, D. H., & Shull, G. E. (1989) *J. Biol. Chem. 264*, 18561–18568.
Cable, M. B., & Briggs, F. N. (1984) *J. Biol. Chem. 259*, 3612–3615.
Campbell, K. P., & McLennan, D. H. (1983) *J. Biol. Chem. 258*, 1391–1394.
Champeil, P., Guillain, F., Venien, C., & Gingold, M. P. (1985) *Biochemistry 24*, 69–81.

Champeil, P., Riollet, S., Orlowski, S., Guillain, F., Seebregts, C. J., & McIntosch, D. B. (1988) *J. Biol. Chem. 263*, 12288–12294.
Clarke, D. M., Maruyama, T. L., Loo, T. W., Leberer, E., Inesi, G., & MacLennan, D. (1989a) *J. Biol. Chem. 264*, 11246–11251.
Clarke, D. M., Loo, T. W., Inesi, G., & MacLennan, D. (1989b) *Nature 339*, 476–478.
Clarke, D. M., Loo, T. W., & MacLennan, D. (1990) *J. Biol. Chem. 265*, 22223–22227.
Clore, G. M., Gronenborn, A. M., Mitchinson, C., & Green, N. M. (1982) *Eur. J. Biochem. 128*, 113–117.
Czarnecki, J., Geahlen, R., & Haley, B. (1979) *Methods Enzymol. 56*, 642–653.
De Meis, L. (1981) in *Transport in Life Sciences* (Bittar, E. E., Ed.) Vol. 2, John Wiley and Sons, New York.
Dupont, Y., Pougeois, R., Ronjat, M., & Verjovski-Almeida, S. (1985) *J. Biol. Chem. 260*, 7241–7249.
Garin, J., Vignais, P. V., Gronenborn, A. M., Clore, G. M., Gao, Z., & Baeuerlein, E. (1988) *FEBS Lett. 242*, 178–182.
Green, N. M. (1989) *Biochem. Soc. Trans. 17*, 970–972.
Green, N. M., & Stokes, D. L. (1991) *Acta Physiol. Scand. 146*, 59–68.
Hoard, D. E., & Ott, D. C. (1965) *J. Am. Chem. Soc. 87*, 1785–1788.
Inesi, G. (1985) *Annu. Rev. Physiol. 47*, 573–601.
Kison, R., Meyer, H. E., & Schoner, W. (1989) *Eur. J. Biochem. 181*, 503–511.
Lacapère, J.-J., Bennett, N., Dupont, Y., & Guillain, F. (1990) *J. Biol. Chem. 265*, 348–353.
Lacapère, J.-J., & Guillain, F. (1992) *Eur. J. Biochem. 211*, 117–126.
Lord, S. T., & Richards, F. M. (1981) *Biochim. Biophys. Acta 649*, 13–23.
MacLennan, D. H. (1989) *J. Biol. Chem. 264*, 13038–13042.
MacLennan, D. H. (1990) *Biophys. J.* 58, 1355–1365.
MacLennan, D. H., Brandl, C. J., Korczak, B., & Green, N. M. (1985) *Nature 316*, 696–700.
Maruyama, K., & McLennan, D. H. (1988) *Proc. Natl. Acad. Sci. U.S.A. 85*, 3314–3318.
Maruyama, K., Clarke, D. M., Fujii, J., Inesi, G., Loo, T. W., & MacLennan, D. (1989) *J. Biol. Chem. 264*, 13038–13042.
McD Stewart, J. M., Jorgensen, P. L., & Grisham, C. M. (1989) *Biochemistry 28*, 4695–4701.
McIntosh, D. B. (1992) *J. Biol. Chem. 267*, 22328–22335.
McIntosh, D. B., Woolley, D. G., & Berman, M. C. (1992) *J. Biol. Chem. 267*, 5301–5309.
Mitchinson, C., Wilderspin, A. F., Trinnaman, B., & Green, N. M. (1982) *FEBS Lett. 146*, 87–92.
Murphy, A. J. (1976) *Biochem. Biophys. Res. Commun. 70*, 1048–1054.
Ovchinnikov, Y. A., Dzhandzugazyan, K. N., Lutsenko, S. V., Mustayev, A. A., & Modyanov, N. N. (1987) *FEBS Lett. 217*, 111–117.
Palmero, I., & Sastre, L. (1989) *J. Biol. Chem. 210*, 737–748.
Rudolf, H. K., Antebi, A., Fink, G. R., Buckley, C. M., Dorman, T. E., LeVitre, J., Davidow, L. S., Mao, J. I., & Moir, D. T. (1989) *Cell 58*, 133–145.
Saito-Naktsuka, K., Yamashita, T., Kubota, I., & Kawakita, M. (1987) *J. Biochem. (Tokyo) 101*, 365–376.
Schlichting, I., Almo, S. C., Rapp, G., Wilson, K., Petratos, K., Lentfer, A., Wittinghofer, A., Kabsch, W., Pai, E. F., Petsko, G. A., & Goody, R. S. (1990) *Nature 345*, 309–315.
Seebregts, C. J., & McIntosh, D. B. (1989) *J. Biol. Chem. 264*, 2043–2052.
Shoshan-Barmatz, V. (1987) *Biochem. J. 247*, 497–504.
Shull, G. E., & Lingrel, J. B. (1986) *J. Biol. Chem. 261*, 16788–16791.
Shull, G. E., & Greeb, J. (1988) *J. Biol. Chem. 263*, 8646–8657.
Shull, G. E., Schwartz, A., & Lingrel, J. B. (1985) *Nature 316*, 691–695.
Stokes, D. L., & Green, N. M. (1990a) *Biophys. J. 57*, 1–14.
Stokes, D. L., & Green, N. M. (1990b) *J. Mol. Biol. 213*, 529–538.
Taylor, W. R., & Green, N. M. (1989) *Eur. J. Biochem. 179*, 241–248.
Toker, A., Ellis, C. A., Sellers, L. A., & Aitken, A. (1990) *Eur. J. Biochem. 191*, 421–429.
Torok, K., Trinnaman, B., & Green, N. M. (1988) *Eur. J. Biochem. 173*, 361–367.
Tran, C. M., Scheiner-Bobis, G., Schöner, W., & Farley, R. A. (1988) *Biophys. J. 53*, 343a.
Tunwell, R. E. A., Conlan, J. W., Matthews, I., East, J. M., & Lee, A. G. (1991) *Biochem. J. 279*, 203–212.
Vilsen, B., Andersen, J., & McLennan, D. (1991) *J. Biol. Chem. 266*, 16157–16164.
Yamamoto, H., Tagaya, M., Fukui, T., & Kawakita, M. (1988) *J. Biochem. 103*, 452–457.
Yamamoto, H., Imamura, Y., Tagaya, M., Fukui, T., & Kawakita, M. (1989) *J. Biochem. 106*, 1121–1125.